Journal of Geoscience and Environment Protection, 2026, 14(9), 213-233
https://www.scirp.org/journal/gep
ISSN Online: 2327-4344
ISSN Print: 2327-4336

Variable-Density Modelling of Groundwater Abstraction, Sea-Level Change and Managed Recharge in the Tudor Coastal Aquifer, Mombasa, Kenya

Charles Ngala Kithome*, Mary Makokha, Shadrack Murimi

Department of Geography, School of Pure and Applied Sciences, Kenyatta University, Nairobi, Kenya
Email: *charliekithome@gmail.com

How to cite this paper: Kithome, C. N., Makokha, M., & Murimi, S. (2026). Variable-Density Modelling of Groundwater Abstraction, Sea-Level Change and Managed Recharge in the Tudor Coastal Aquifer, Mombasa, Kenya. *Journal of Geoscience and Environment Protection, 14,* 213-233.
https://doi.org/10.4236/gep.2026.149012

Received: August 20, 2026
Accepted: September 25, 2026
Published: September 28, 2026

Abstract

Coastal groundwater management requires models that can distinguish the individual and combined effects of groundwater abstraction, a changing saline coastal boundary, and interventions that preserve freshwater head. A companion hydrochemical and statistical assessment of the Tudor aquifer, Mombasa County, Kenya (Kithome, Makokha, & Murimi, 2026) established strong empirical associations between licensed groundwater abstraction, local relative sea-level change, hydraulic-head decline and chloride concentration, but, being observational, could not simulate the aquifer's process-based response to future stress or to candidate management interventions. This study addresses the gap by developing a calibrated two-dimensional SEAWAT variable-density flow and chloride-transport model for the Tudor aquifer, using the Ghyben-Herzberg relation only as a first-order analytical screening check. The 8-km cross-section comprised 80 columns and 20 layers (1600 active cells), with a specified coastal head and seawater-concentration boundary, a no-flow Precambrian basement, spatially distributed recharge, and 15 represented pumping centres. Calibration used hydraulic head at eight monitoring boreholes and chloride observations from 30 groundwater records. Hydraulic-head calibration yielded RMSE = 0.38 m, MAE = 0.29 m and R^2 = 0.89; chloride calibration yielded RMSE = 892 mg/L, MAE = 671 mg/L and R^2 = 0.94. Under the 2025 reference condition (+0.23 m relative coastal head, 11,500 m^3/day represented pumping and 150 mm/year mean recharge), coastal chloride was 12,847 mg/L, the 5000 mg/L isochlor occurred about 2.5 km inland of the coast and the 1000 mg/L isochlor about 5.5 km inland of the coast. Reducing represented pumping by 30% (to 8050 m^3/day) moved the system in a freshwater-preserving direction, and managed recharge to 650 mm/year in designated zones produced the largest simulated improvement, reducing coastal chloride from 12,847 mg/L to approximately 7837 mg/L (about 39% lower). A higher coastal-head condition (+0.50 m, giving +0.73 m relative coastal head) and a combined-stress scenario (represented pumping raised to 14,000 m^3/day, recharge reduced by 20% to 120 mm/year, and coastal head raised to +0.73 m) both moved the system toward greater intrusion, with the combined-stress scenario producing the largest deterioration and shifting the 5000 mg/L chloride front from 2.50 km to approximately 4.54 km inland of the coast (an advance of about 2.04 km). Sensitivity tests varying hydraulic conductivity and dispersivity by ±20% changed simulated chloride by approximately 15% - 25% but did not change the ranking of scenarios by direction of response. As an independent, qualitative consistency check—not a transient 2015-2025 simulation, since the model is calibrated to 2025 conditions and each scenario is run to steady state—the 2025 reference simulation's implied head and chloride levels are broadly consistent in direction and order of magnitude with the 0.80 m hydraulic-head decline and 2565 mg/L coastal chloride increase reported between 2015 and 2025 in the companion study. The results show that preserving freshwater head through coordinated abstraction control and carefully monitored managed recharge offers a stronger management response than treating sea-level change or pumping in isolation. The model is intended for comparative scenario assessment rather than parcel-scale prediction or deterministic forecasting.

Keywords

SEAWAT, Variable-Density Flow, Seawater Intrusion, Groundwater Abstraction, Managed Recharge, Sea-Level Change, Ghyben-Herzberg, Tudor Aquifer, Mombasa

1. Introduction

1.1. Coastal Aquifers and Seawater Intrusion

Seawater intrusion is a density-dependent groundwater process in which saline water migrates into coastal freshwater systems when the hydraulic balance between inland recharge, groundwater discharge and the marine boundary is disturbed. Groundwater abstraction lowers freshwater head and can induce lateral migration and local upconing, while a higher coastal boundary increases pressure from the saline side. These mechanisms may act simultaneously and can be intensified by aquifer heterogeneity, preferential flow and reduced recharge (Werner et al., 2013; Gopinath et al., 2019; Hingst et al., 2024). The management problem is particularly acute in rapidly urbanizing coastal aquifers, where groundwater demand can increase faster than monitoring and regulatory capacity, and where the freshwater-saltwater transition must be understood well enough to test candidate interventions before they are implemented at scale.

1.2. From Sharp-Interface Theory to Variable-Density Simulation

The Ghyben-Herzberg relationship provides a first-order estimate of the depth of the freshwater-saltwater interface below sea level from freshwater head above sea level. Its hydrostatic, homogeneous, sharp-interface assumptions make it useful for rapid conceptual screening but insufficient for a pumped, dispersive and heterogeneous coastal aquifer (Pool & Carrera, 2011; Llopis-Albert & Pulido-Velázquez, 2014). The relation is expressed as

$$z = \left[\rho f / \left(\rho s - \rho f\right)\right] h \tag{1}$$

where z is the depth of the freshwater-saltwater interface below sea level, h is freshwater head above sea level, ρf is freshwater density and ρs is seawater density. Using $\rho f = 1000\ \text{kg/m}^3$ and $\rho s = 1025\ \text{kg/m}^3$ gives

$$z = 40h \tag{2}$$

indicating that every metre of freshwater head above sea level corresponds to approximately 40 m of interface depth below sea level. This 40:1 ratio has substantial management implications, because small pumping-induced reductions in freshwater head can translate into large upward and landward movements of the interface. Pool and Carrera (2011) proposed a correction factor that incorporates dispersivity and hydraulic gradient to account for the mixing zone omitted by the sharp-interface assumption,

$$zm = 40h - \delta \tag{3}$$

where δ is a correction term dependent on dispersivity and hydraulic gradient. Despite these limitations, Ghyben-Herzberg screening remains useful because it communicates aquifer vulnerability intuitively, enables rapid first-order assessment without a numerical model, and provides an independent benchmark against which a variable-density simulation can be compared (Mantoglou, 2003).

Real coastal aquifers, however, are characterized by dynamic flow and a transition zone of mixed freshwater and saltwater rather than a sharp interface (Meyer et al., 2019). Variable-density flow theory describes these systems through coupled conservation equations for fluid mass and solute mass. The flow equation, modified from the standard groundwater-flow equation to account for density variation, is

$$\nabla \cdot \left\{\rho K \left[\nabla h + \left(\rho - \rho f\right)/\rho f \nabla z\right]\right\} = \rho Ss\left(\partial h/\partial t\right) + \theta\left(\partial \rho/\partial t\right) \tag{4}$$

where ρ is fluid density, K is the hydraulic conductivity tensor, h is hydraulic head, z is elevation, Ss is specific storage, θ is porosity and t is time; the term $\left(\rho - \rho f\right)/\rho f \nabla z$ represents the density-driven flow component. The associated solute-transport equation is

$$\partial\left(\theta C\right)/\partial t = \nabla \cdot \left(\theta D \nabla C\right) - \nabla \cdot \left(qC\right) + Qs \tag{5}$$

where C is solute concentration, D is the hydrodynamic dispersion tensor, q is the specific discharge vector and Qs represents solute sources or sinks. These coupled, nonlinear equations generally require numerical solution. SEAWAT couples MODFLOW, for groundwater flow, with MT3DMS, for solute transport, and solves the equations using finite-difference methods, allowing the dispersive transition zone, pumping-induced upconing and transient response to imposed stress to be represented explicitly—none of which are captured by Ghyben-Herzberg screening or by correlation analysis of field observations (El Hamidi et al., 2021; Akhtar et al., 2022).

1.3. Global Evidence from SEAWAT Applications in Coastal Aquifers

SEAWAT and comparable variable-density codes have been applied to quantify seawater-intrusion drivers and to test management scenarios in a wide range of coastal settings. Abd-Elaty, Javadi, and Abd-Elhamid (2021) used SEAWAT to compare management options for the Nile Delta aquifer, Egypt, and found that increased artificial recharge produced greater retardation of intrusion (19.5%) than reduced pumping alone (6.2%), while combined measures gave the largest reduction (21.3%)—a pattern of recharge outperforming an equivalent-direction pumping reduction that recurs in several subsequent studies, including the present one. Tran et al. (2022) developed a three-dimensional SEAWAT model of the Mekong Delta, Vietnam, calibrated and validated over multiple years, and projected that continued overextraction would drive salinity above 2.0 g/L to depths of approximately 150 m and several kilometres inland within 20 - 30 years without intervention. Akhtar, Sana, Tauseef, and Tanaka (2022) modelled the Wadi Al-Jizi coastal aquifer, Oman, with MODFLOW coupled to MT3DMS, projecting that continued abstraction at current rates would allow highly saline water (TDS > 12,800 mg/L) to transgress approximately 0.8 km inland by 2040, while a 30% pumping reduction combined with artificial recharge stabilized the interface. El Hamidi, Larabi, and Faouzi (2021) modelled the Rmel-Oulad Ogbane aquifer, Morocco, under combined climate-change and sea-level-rise scenarios to 2040, projecting the intrusion toe reaching approximately 5.2 km inland at 15 - 25 g/L compared with 3.8 km under baseline conditions, a 36% increase in intrusion distance attributable to the combined stress. Agossou, Yang, and Lee (2022) calibrated a three-dimensional SEAWAT model of Benin's coastal aquifer system for 2015-2020 and reported a 1.65 m freshwater-head decline and a 1.92 km^2 increase in intrusion area over the five-year baseline, with recharge able to offset moderate sea-level rise but combined interventions required under high-end scenarios. Narayanan and Eldho (2024) reported a counterintuitive management insight—that pumping brackish water from the saline zone itself can create a hydraulic barrier that restrains further seawater advance—while Hingst et al. (2024) demonstrated that the spatial distribution of pumping, not only its total volume, controls intrusion severity, with pumping concentrated near tidal streams causing disproportionately greater salinization than the same total pumping distributed inland.

Model calibration and validation are central to the credibility of these applications. Meyer, Engesgaard, and Sonnenborg (2019) demonstrated multi-objective SEAWAT calibration against hydraulic head, borehole salinity profiles and airborne electromagnetic data, and argued that model adequacy should be judged against data resolution, intended use, residual pattern and sensitivity rather than a universal percentage threshold—an approach followed in the present study, which reports full calibration statistics and restricts inference to comparative scenario response rather than parcel-scale prediction.

1.4. Sea-Level Change and Combined Stress

Sea-level rise increases coastal hydraulic loading and can reduce the seaward freshwater gradient that resists saline encroachment, raise the base level for groundwater discharge, and enhance tidal intrusion through creeks and estuaries (Cao et al., 2024; Hingst et al., 2024). The Intergovernmental Panel on Climate Change (2021) assessed a likely global mean sea-level rise of 0.44 - 0.76 m under SSP 2 - 4.5 and 0.63 - 1.01 m under SSP5-8.5 for 2081-2100 relative to 1995-2014, though regional expression also depends on ocean dynamics, gravitational effects and vertical land movement, which is why the present study treats its local tide-gauge record as a relative coastal-boundary anomaly rather than a proxy for the global rate. Cao, Guo, and Liu (2024) combined physical sandbox experiments with two-dimensional SEAWAT simulation and found that sea-level rises of only a few centimetres measurably expanded the saline wedge, and that superimposed groundwater extraction greatly intensified vertical intrusion—the combined effect of sea-level rise and pumping being more severe than either stress alone. This finding motivates explicit combined-stress scenario testing rather than evaluating abstraction and coastal-boundary change as independent management narratives, an approach adopted directly in the present study's scenario design.

1.5. Evidence from Kenya and the East African Coast

Research on seawater intrusion along the Kenyan coast has grown over the past decade. Oiro and Comte (2019) documented intrusion pathways, aquifer heterogeneity and pumping sensitivity in a stressed aquifer of southern coastal Kenya, and Makokha (2019) described hydrochemical groundwater-quality variation along the Kenyan coastal region. Farther afield, Mtoni et al. (2013) documented saltwater intrusion and nitrate pollution in the coastal aquifer of Dar es Salaam, Tanzania, illustrating that comparable East African coastal aquifers are vulnerable where abstraction interacts with marine hydraulic boundaries and heterogeneous coastal geology. These studies establish the regional pattern but do not substitute for a locally resolved, numerically modelled assessment of the Tudor aquifer specifically. A companion study (Kithome, Makokha, & Murimi, 2026) addressed the hydrochemical and statistical component of this gap for Tudor, establishing that groundwater is measurably more saline toward the coast and Tudor Creek, that licensed abstraction rose by approximately 133% between 2015 and 2025 while mean freshwater head declined by 0.80 m, and that both licensed abstraction and the local relative sea-level anomaly were strongly and independently associated with rising chloride concentration.

1.6. The Tudor Aquifer: Setting and Knowledge Gap

The Tudor aquifer, Mombasa County, is hydraulically connected to the Indian Ocean and Tudor Creek and is developed for domestic, commercial and industrial groundwater supply. The aquifer is hosted mainly in coastal sedimentary units including coral sands, coral limestone and calcareous sandstone over low-permeability basement. Fracturing and dissolution enhance permeability in the limestone, while clay lenses and variable lithology create local heterogeneity. Previous work along the East African coast demonstrates that pumping, marine boundaries and heterogeneous geology can combine to accelerate salinization (Mtoni et al., 2013; Oiro & Comte, 2019; Makokha, 2019).

The companion hydrochemical and statistical assessment established strong coast-normal salinity gradients and quantified relationships among abstraction, hydraulic head, local relative sea level and chloride, but, being an observational analysis of correlation and regression, could not simulate the aquifer's response to conditions that have not yet occurred, nor be used directly to test the likely effect of a specific management intervention such as staged pumping reduction or a managed-recharge scheme. This is an important limitation for a rapidly urbanizing aquifer such as Tudor, where the Water Resources Authority and Mombasa County require a defensible, process-based basis for evaluating abstraction control and recharge options before they are implemented (Republic of Kenya, 2016).

1.7. Objectives

This study addresses that gap by developing, calibrating and applying a two-dimensional variable-density SEAWAT model of the Tudor aquifer. The specific objectives were to: 1) construct and calibrate the model against independent 2025 hydraulic-head and chloride observations; 2) reproduce, as an independent check, the observed 2015-2025 hydraulic-head decline and coastal chloride increase; 3) quantify the 2025 reference position of the chloride front and benchmark it against analytical Ghyben-Herzberg screening; and 4) compare the modelled aquifer response under a pumping-control scenario, a managed-recharge scenario, a higher coastal-head scenario and a combined-stress scenario, in order to identify management measures that preserve freshwater head under increasing coastal stress.

2. Materials and Methods

2.1. Study Area and Hydrogeological Setting

The Tudor aquifer study area lies in Mombasa County on the Kenyan Indian Ocean coast at approximately 4˚03'S, 39˚40'E. The modelling section extends from inland Tudor toward Tudor Creek and the Indian Ocean, which constitute the principal saline hydraulic boundaries represented in the model. Mombasa County is Kenya's second-largest urban centre and principal seaport, with a population of approximately 1.2 million (Kenya National Bureau of Statistics, 2019), and the aquifer area encompasses industrial zones (Changamwe, Shimanzi), residential neighbourhoods (Tudor, Mlaleo, Mikindani) and peri-urban agricultural land.

The coastal setting has low relief and a tropical climate, with long rains from March to May and short rains from October to December, high potential evapotranspiration, and seasonally variable rainfall. Because a measured Tudor water balance was not available, recharge was treated as a calibrated model input rather than inferred directly from rainfall. Borehole-log synthesis indicates shallow coral sand and beach deposits, a productive coral-limestone interval, locally interbedded calcareous sandstone and clay, and low-permeability Precambrian basement. The limestone contains secondary porosity from fracturing and dissolution, creating preferential pathways and spatially variable hydraulic conductivity. Under unstressed conditions, groundwater flows from inland areas toward the coast and Tudor Creek; this seaward freshwater discharge provides the hydraulic resistance to saline encroachment that abstraction and coastal-head rise progressively erode (Oiro & Comte, 2019).

2.2. Data Used for Model Construction and Calibration

The model integrated three evidence streams. This multi-evidence calibration strategy follows the broader coastal-aquifer modelling principle that hydraulic head, salinity and hydrostratigraphic information should be interpreted jointly rather than relying on a single calibration target (Meyer et al., 2019; Werner et al., 2013). First, available Water Resources Authority records provided licensed groundwater abstraction and monitoring hydraulic-head information for 2015-2025. Second, local relative sea-level observations for 2015-2025 were obtained from the Mombasa II/Kilindini Harbour tide and telemetric gauge record (Kenya Ports Authority, unpublished data, 2015-2025). Third, the 2025 hydrochemical dataset comprised 30 groundwater records used to constrain the coast-to-inland chloride distribution, of which eight monitoring boreholes also provided the hydraulic-head calibration targets. These datasets were treated according to their different temporal and spatial supports rather than as a single continuously monitored panel (Water Resources Authority, 2025), consistent with the data-governance approach used in the companion hydrochemical and statistical study.

2.3. SEAWAT Model Domain and Boundary Conditions

A two-dimensional vertical SEAWAT cross-section was constructed along an inland-to-coast transect (A-A′) from inland Tudor to the coastal boundary (**Figure 1**). The model domain extended 8 km inland and was discretized into 80 columns and 20 layers, giving 1600 active cells representing, from top to bottom, surficial deposits, the coral-limestone aquifer, weathered sandstone/siltstone, clay/silt lenses and the Precambrian basement. Specified head and seawater concentration were assigned at the coastal boundary and allowed to vary with the local relative sea-level record; the Precambrian basement was represented as a no-flow lower boundary; spatially distributed recharge entered through the upper boundary; and licensed abstraction was allocated to 15 major pumping centres distributed across the section. The represented pumping total was distinguished throughout from the aquifer-wide licensed total because pumping centres outside the cross-section were not assigned to model cells.

Represented pumping and recharge volumes were converted to per-unit-length inputs for the two-dimensional section using an assumed effective aquifer width of 1.0 km along transect A-A′. The 15 pumping centres and the hydraulic-head/chloride observation points were assigned to their nearest model column by perpendicular projection onto the transect line. Each scenario, including the 2025 reference condition, was run as an independent steady-state simulation, using a single stress period carried to hydraulic and solute-transport convergence rather than a time-stepped transient simulation. Initial heads and concentrations were based on a hydrostatic starting estimate, with scenario initialization refined using the calibrated 2025 reference solution. The inland (landward, x = 0) boundary was represented as a no-flow boundary, consistent with the interpreted inland extent of the Tudor aquifer's active flow system.

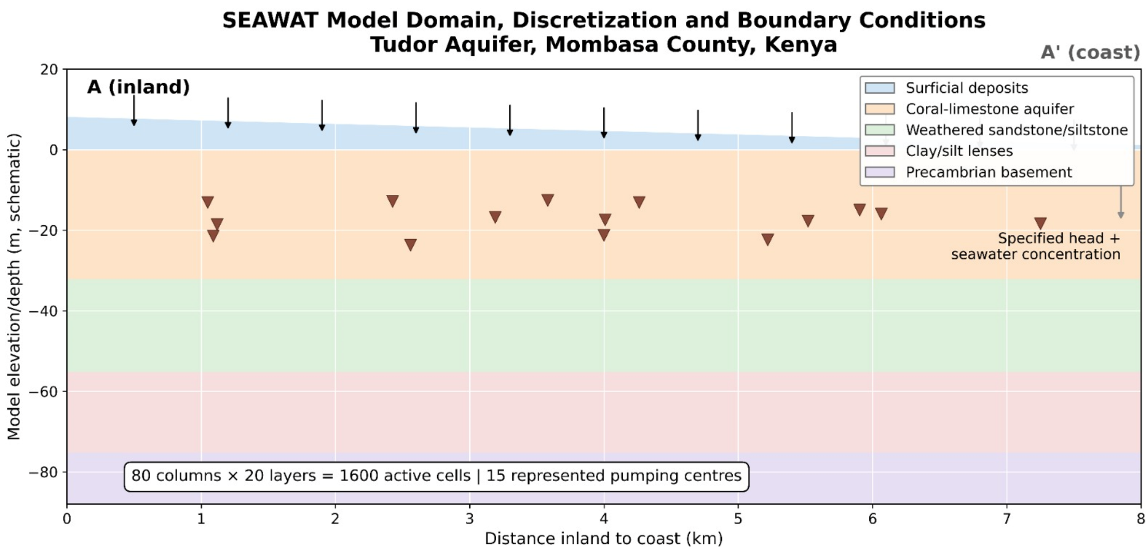

Figure 1. SEAWAT model domain, discretization and boundary conditions for the two-dimensional Tudor cross-section.

2.4. Calibration, Performance Criteria and Reference Condition

Calibration involved adjustment of hydraulic conductivity, porosity, dispersivity and recharge within hydrogeologically plausible ranges. The approach is consistent with published variable-density studies in which flow parameters are first constrained by head and then transport parameters are refined against salinity observations, with model adequacy judged from multiple diagnostics rather than one goodness-of-fit statistic (Meyer et al., 2019; El Hamidi et al., 2021; Akhtar et al., 2022). Simulated hydraulic head was compared with observations from eight monitoring boreholes, while simulated chloride was compared with the 30 groundwater chloride observations positioned along the cross-section using recorded coastline distance. Performance was evaluated using graphical agreement with the 1:1

line, root mean square error (RMSE), mean absolute error (MAE), coefficient of determination (R^2) and bias. The calibrated horizontal hydraulic conductivity was 28 m/day, with zonal values of approximately 15 - 45 m/day; vertical hydraulic conductivity was 2.8 m/day, longitudinal dispersivity 35 m and transverse dispersivity 3.5 m. Mean recharge was 150 mm/year, with a spatial calibration range of approximately 120 - 180 mm/year. The 2025 reference simulation used a +0.23 m local relative coastal-head condition and represented 11,500 m^3/day of licensed abstraction distributed among the 15 pumping centres within the two-dimensional section.

All eight hydraulic-head observations and all 30 chloride observations from the 2025 campaign were used in calibration; none were withheld as a temporal validation subset. The comparison against 2015-2025 change reported in Sections 2.7 and 3.5 is therefore an independent, external consistency check against the companion hydrochemical and statistical study's regression-based trend estimates, not a held-out validation dataset drawn from the same 2025 monitoring network.

2.5. Ghyben-Herzberg Screening Method

The Ghyben-Herzberg relation was retained as an analytical screening benchmark rather than a substitute for variable-density simulation, following Equations (1) - (3). This relation assumes hydrostatic equilibrium, a sharp interface and homogeneous conditions; it does not represent dispersion, pumping-induced upconing or the finite transition zone simulated by SEAWAT (Pool & Carrera, 2011; Llopis-Albert & Pulido-Velázquez, 2014).

2.6. Stress and Management Scenario Design

Five deterministic experiments were compared: the calibrated 2025 reference condition; pumping control; managed recharge; a higher coastal-head condition; and combined stress (**Table 1**). The 2025 reference used a +0.23 m local relative coastal-head condition, 11,500 m^3/day of represented licensed pumping and mean recharge of 150 mm/year. Pumping control reduced represented pumping by 30%, to 8050 m^3/day. Managed recharge increased recharge to 650 mm/year in designated inland zones. The higher coastal-head case imposed +0.50 m relative coastal head (giving +0.73 m absolute relative coastal head). The combined-stress case raised represented pumping to 14,000 m^3/day (+21.7% relative to the reference), reduced recharge by 20% to 120 mm/year, and raised relative coastal head to +0.73 m, applying all three changes jointly rather than altering any single driver in isolation. Outputs were compared using freshwater-head response, chloride concentration and chloride-front position. Scenario outputs are reported directly as these raw quantities—mean freshwater head (m), coastal chloride (mg/L) and 5000 mg/L chloride-front position (km inland of the coast) relative to the 2025 reference simulation—rather than as a weighted or normalized composite index. No composite index is reported because it would require a normalization and weighting scheme across variables of different units that this study does not define; the direction of each scenario's response (toward or away from freshwater preservation) is unambiguous from the sign of these raw changes. The experiments are comparative model responses, not deterministic forecasts.

Table 1. Specification of the 2025 reference condition and the four stress and management scenarios.

Scenario	Specified change	Represented pumping	Recharge	Relative coastal head
2025 reference	Calibrated reference condition	11,500 m^3/day	150 mm/yr	+0.23 m
Pumping control	Represented pumping −30%	8050 m^3/day	150 mm/yr	+0.23 m
Managed recharge	Recharge raised in designated inland zones	11,500 m^3/day	650 mm/yr	+0.23 m
Higher coastal head	Relative coastal head +0.50 m	11,500 m^3/day	150 mm/yr	+0.73 m
Combined stress	Pumping 14,000 m^3/day; recharge −20% (120 mm/yr); coastal head +0.73 m	14,000 m^3/day (+21.7%)	120 mm/yr (−20%)	+0.73 m

2.7. Sensitivity Analysis and Independent Verification

Two additional checks assessed model robustness beyond calibration fit. First, sensitivity tests varied hydraulic conductivity and dispersivity by ±20% from their calibrated values and examined the resulting change in simulated chloride concentration and in the ranking of the four scenarios by direction of response. Second, as an independent, qualitative consistency check not used in calibration, the direction and approximate magnitude of the calibrated 2025 reference model's implied change relative to earlier, less-saline conditions were compared with the observed 2015-2025 hydraulic-head decline (0.80 m) and coastal chloride increase (2565 mg/L) reported in the companion hydrochemical and statistical study. Because the SEAWAT model here is run to steady state for each scenario rather than as a transient 2015-2025 simulation, this comparison establishes broad plausibility of direction and order of magnitude, not a reproduced time series, and should not be read as formal temporal validation.

3. Results

3.1. Calibration Performance

Hydraulic-head calibration produced RMSE = 0.38 m, MAE = 0.29 m, R^2 = 0.89 and bias = +0.07 m. Chloride calibration produced RMSE = 892 mg/L, MAE = 671 mg/L, R^2 = 0.94 and bias = +176 mg/L (Table 2). The corresponding calibration diagnostics for hydraulic head and chloride concentration are shown in Figure 2. The small positive head bias indicates limited systematic error in simulated heads, while the chloride bias indicates a slight average overprediction of salinity. The model reproduces the principal inland-to-coastal hydraulic and salinity gradients sufficiently for scenario comparison, but the heterogeneous two-dimensional representation is not intended for parcel-scale prediction.

Table 2. Calibration performance summary, 2025 reference simulation.

Target	n	RMSE	MAE	R^2	Bias
Hydraulic head (m)	8	0.38 m	0.29 m	0.89	+0.07 m
Chloride (mg/L)	30	892 mg/L	671 mg/L	0.94	+176 mg/L

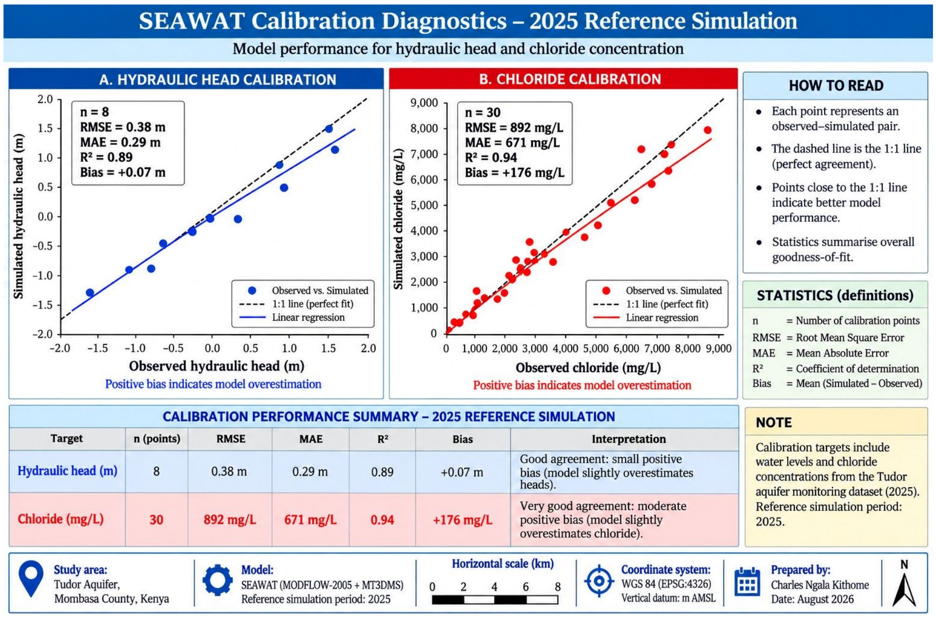

Figure 2. SEAWAT calibration diagnostics for hydraulic head (n = 8) and chloride concentration (n = 30).

3.2. 2025 Reference Simulation

Table 3. Model outputs under 2025 reference conditions.

Output	Value	Interpretation
Mean hydraulic head	4.43 m asl	Reference freshwater head
Coastal chloride (0 - 1 km inland from coast)	12,847 mg/L	Severely saline coastal model zone
Intermediate chloride (3 - 5 km inland from coast)	3256 mg/L	Active transition zone
Inland chloride (>5 km inland from coast)	1124 mg/L	Low-level saline influence persists
5000 mg/L isochlor	2.5 km inland	High-salinity front
1000 mg/L isochlor	5.5 km inland	Lower-salinity transition
250 mg/L isochlor	Beyond 8 km domain	Extends beyond model boundary
Ghyben-Herzberg screening depth	177.2 m below sea level	Analytical screening only

The reference simulation produced coastal chloride of 12,847 mg/L, with the 5000 mg/L isochlor approximately 2.5 km inland of the coast (equivalently, about 5.5 km from the inland, x = 0, boundary of the section) and the 1000 mg/L isochlor approximately 5.5 km inland of the coast (about 2.5 km from the inland boundary) (Table 3; Figure 3). The 250 mg/L isochlor extended beyond the 8-km inland limit of the modelled domain, indicating that low-level chloride influence persisted throughout the represented section under reference conditions. These are model-domain results constrained by the two-dimensional geometry, calibration data and specified boundary conditions.

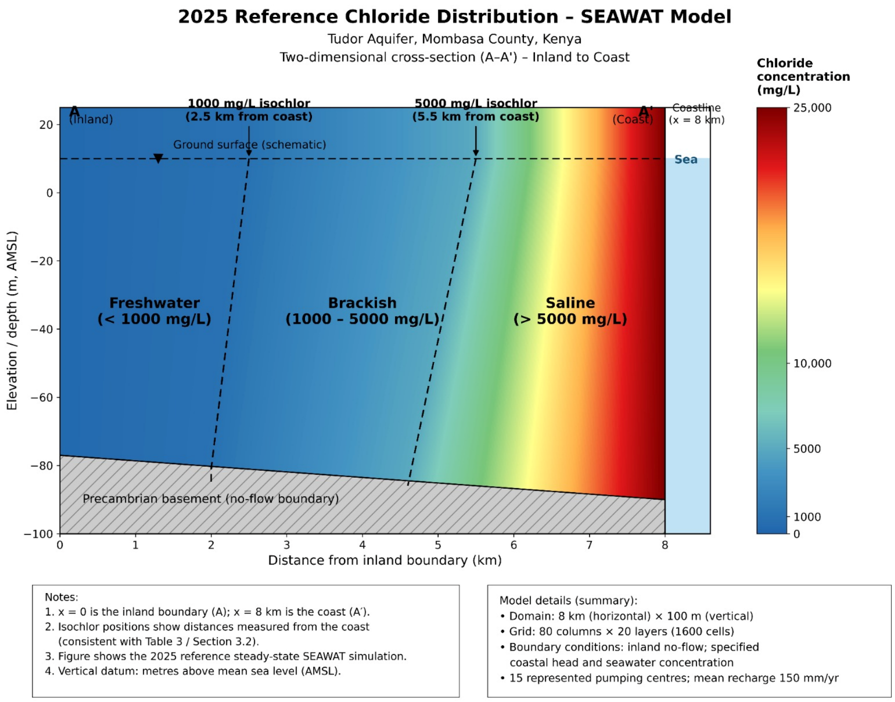

Figure 3. Model-based representation of the 2025 reference chloride transition and reported 1000 mg/L and 5000 mg/L isochlor positions.

3.3. Ghyben-Herzberg Screening Results

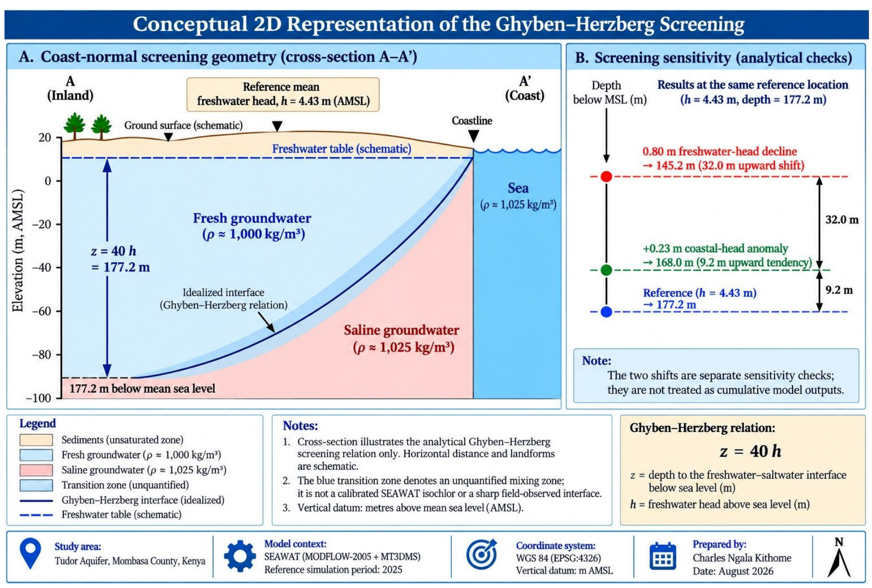

Figure 4. Conceptual Ghyben-Herzberg screening geometry and separate head-sensitivity checks at the reference mean freshwater head (h = 4.43 m).

At the reference mean freshwater head of 4.43 m, the Ghyben-Herzberg approximation gives a screening interface depth of approximately 177.2 m below sea level (Figure 4). Applied as separate first-order sensitivity checks at this reference location, the observed 0.80 m freshwater-head decline corresponds to an idealised interface-depth shift of approximately 32 m, and a 0.23 m increase in coastal head, freshwater head held constant, corresponds to an approximate 9.2 m reduction in relative freshwater-head support. These are analytical sensitivity calculations, not cumulative SEAWAT outputs, and must not be added together or interpreted as SEAWAT-predicted interface movements.

3.4. Scenario Responses

The five scenarios produced clearly differentiated freshwater responses, reported as directly interpretable model quantities rather than as a weighted composite index (Table 4). Reducing represented pumping by 30% (to 8050 m^3/day) moved the system in a freshwater-preserving direction. Managed recharge to 650 mm/year in designated inland zones generated the largest quantified improvement, reducing coastal chloride from 12,847 mg/L to approximately 7837 mg/L (about 39% lower). In contrast, the higher coastal-head condition (+0.50 m above the 2025 coastal-head condition, giving +0.73 m relative coastal head) moved the system toward greater intrusion. The combined-stress scenario (pumping 14,000 m^3/day, recharge reduced by 20% to 120 mm/year, and coastal head +0.73 m) produced the largest deterioration, moving the 5000 mg/L chloride front from 2.50 km to approximately 4.54 km inland of the coast, an advance of about 2.04 km. Where raw scenario-specific head or chloride values were not retained in the available output summary, the manuscript reports only the supported direction of response and does not infer unreported magnitudes.

Table 4. SEAWAT scenario responses relative to the 2025 reference simulation.

Scenario	Specified change	Raw response vs. 2025 reference	Main result
2025 reference	+0.23 m coastal head; 11,500 m^3/day pumping; 150 mm/yr recharge	Reference	Head 4.43 m; coastal Cl^- 12,847 mg/L
Pumping control	Pumping −30% to 8050 m^3/day	Direction: freshwater-preserving; raw scenario-specific Δ head and Δ coastal chloride not reported	Freshwater head preserved; intrusion pressure reduced
Managed recharge	Recharge to 650 mm/yr in designated zones	Coastal Cl^- reduced from 12,847 to ≈7837 mg/L (−39%)	Coastal chloride −39%; largest improvement
Higher coastal head	Relative coastal head +0.50 m	Direction: freshwater-preserving; raw scenario-specific Δ head and Δ coastal chloride not reported	Landward pressure and salinity increased
Combined stress	Pumping 14,000 m^3/day; recharge −20% (120 mm/yr); coastal head +0.73 m	5000 mg/L front 2.50 → ≈4.54 km inland of coast (+2.04 km)	5000 mg/L front advanced 2.04 km inland

3.5. Independent Checks and Sensitivity

As a qualitative, direction-and-magnitude consistency check rather than a reproduced transient time series (the model is run to steady state, not as a 2015-2025 transient simulation—see Sections 2.3 and 2.7), the calibrated 2025 reference model's implied change relative to earlier conditions is broadly consistent with the observed 0.80 m hydraulic-head decline and 2565 mg/L coastal chloride increase reported between 2015 and 2025 in the companion study. Sensitivity tests varying hydraulic conductivity and dispersivity by ±20% changed simulated chloride by approximately 15% - 25% but did not alter the ranking of scenarios by direction of response. This stability is important because it indicates that the relative management conclusions are less sensitive than the exact predicted chloride concentrations to plausible parameter uncertainty.

4. Discussion

4.1. Abstraction as a Controllable Hydraulic Stress

The pumping-control experiment demonstrates the direct management value of preserving freshwater head. A 30% reduction in represented pumping moved the freshwater response in the improving direction. The available scenario summary supports the direction of this response but does not provide a separate raw mean-head or coastal-chloride change for this experiment; no unreported magnitude is therefore inferred. This direction is consistent with coastal-aquifer theory and modelling studies showing that excessive pumping lowers inland head, weakens seaward discharge and promotes lateral intrusion and upconing (Mantoglou, 2003; Tran et al., 2022; Narayanan & Eldho, 2024). In Tudor, the result is especially relevant because licensed abstraction increased substantially during the monitoring period while mean hydraulic head declined.

The model should not be interpreted as prescribing an immediate uniform 30% cut across all users. The cross-section contains 15 represented pumping centres and does not include every licensed abstraction point in the aquifer. A practical application would therefore require staged reduction targets, metering, head and chloride trigger levels, and spatial prioritization of pumping centres that have the greatest hydraulic influence on the coastal transition zone.

4.2. Managed Recharge as a Head-Preservation Measure

Managed recharge produced the strongest beneficial response, reducing coastal chloride from 12,847 mg/L to approximately 7837 mg/L (about 39% lower). The mechanism is hydraulic: additional freshwater recharge increases inland head and strengthens the seaward gradient, thereby resisting saline migration. Comparable variable-density studies show that recharge enhancement can be more effective than an equivalent-direction pumping reduction when appropriately located and when the added recharge is not immediately offset by increased abstraction (Abd-Elaty et al., 2021; Akhtar et al., 2022)—a pattern consistent with the present scenario ranking. Because a raw pumping-control coastal-chloride change was not retained in the available output summary, the comparison is stated by direction and ranking rather than by an unsupported numerical difference.

The scenario represents a modelling experiment rather than a ready-to-build recharge scheme. Recharge to 650 mm/year in designated zones must therefore be tested through a monitored pilot before scale-up. Source-water quality, infiltration capacity, clogging, land availability, groundwater mounding, possible mobilization of contaminants, and the hydraulic connection to existing wells should all be assessed. Pumping control should remain in place during a pilot so that the recharge signal can be distinguished from changes in abstraction.

4.3. Higher Coastal Head and Combined Stress

The higher coastal-head experiment moved the system toward greater intrusion, while combined stress (pumping raised to 14,000 m^3/day, recharge reduced 20% to 120 mm/year, coastal head raised to +0.73 m) caused the largest deterioration and shifted the 5000 mg/L front 2.04 km farther inland (from 2.50 km to approximately 4.54 km inland of the coast). These results illustrate why sea-level change and abstraction should not be treated as independent management narratives. A higher saline-side boundary reduces the freshwater-to-coastal hydraulic contrast, while pumping simultaneously lowers the inland freshwater head. When both act together, the transition zone responds more strongly than under either pressure alone, consistent with variable-density studies of sea-level-rise and pumping interactions (Agossou et al., 2022; Cao et al., 2024; Hingst et al., 2024).

4.4. Why the Ghyben-Herzberg Relation Is Only a Screening Tool

The Ghyben-Herzberg calculation is useful because it communicates the sensitivity of a coastal freshwater lens to changes in head. However, its sharp-interface and hydrostatic assumptions are poorly suited to an urban, pumped and heterogeneous coastal aquifer. The Tudor model includes a transition zone, density-dependent transport, dispersion and pumping stresses that the analytical relation cannot represent. The 177.2 m screening depth therefore should not be presented as an observed interface depth. Its value in this study is diagnostic: it demonstrates that even modest head losses can correspond to large first-order changes in freshwater support, reinforcing the need for a variable-density model (Pool & Carrera, 2011; Llopis-Albert & Pulido-Velázquez, 2014).

4.5. Comparison with Regional and Global SEAWAT Applications

The direction and, in several cases, the approximate order of magnitude of the Tudor results are consistent with SEAWAT-based findings from other tropical and sub-tropical coastal aquifers (**Table 5**). Abstraction and coastal-head increase promote intrusion, while pumping reduction and, more strongly, managed recharge restrain it—the same pattern reported for the Nile Delta, where recharge outperformed pumping reduction (Abd-Elaty et al., 2021), and for Wadi Al-Jizi, Oman, where combined pumping reduction and recharge stabilized the interface

(Akhtar et al., 2022). The 2.04 km inland advance of the 5000 mg/L front under combined stress in the Tudor cross-section is an order of magnitude smaller than the multi-kilometre fronts reported for the Mekong Delta under prolonged over-extraction (Tran et al., 2022) and for Morocco's Rmel-Oulad Ogbane aquifer under combined climate and pumping stress (El Hamidi et al., 2021), which is plausible given Tudor's shorter simulation period, smaller domain and comparatively lower represented pumping. Direct numerical comparison remains limited by differences in aquifer geometry, hydraulic properties, simulation period and stress magnitude across these studies.

Table 5. Comparative summary of SEAWAT-based intrusion and management responses in coastal aquifers.

Study/location	Approach	Key quantified finding
Tudor aquifer, Kenya (this study)	2-D SEAWAT, 5 scenarios	Pumping −30% (8050 m^3/day): freshwater-preserving direction (directional response; raw Δ not reported); managed recharge (650 mm/yr): coastal Cl^- reduced from 12,847 to ≈7837 (−39%); coastal head +0.50 m: intrusion-worsening direction (directional response; raw Δ not reported); combined stress (pumping 14,000 m^3/day, recharge −20%, coastal head +0.73 m): 5000 mg/L front 2.50 → ≈4.54 km inland (+2.04 km)
Nile Delta, Egypt (Abd-Elaty et al., 2021)	SEAWAT well-system scenarios	Recharge: 19.5% retardation; pumping reduction: 6.2%; combined: 21.3%
Mekong Delta, Vietnam (Tran et al., 2022)	3-D SEAWAT, multi-year calibration	Overextraction drives >2.0 g/L salinity ~150 m deep, several km inland within 20 - 30 yrs
Wadi Al-Jizi, Oman (Akhtar et al., 2022)	MODFLOW + MT3DMS	Unchanged abstraction: TDS > 12,800 mg/L reaches ~0.8 km inland by 2040; 30% cut + recharge stabilizes interface
Rmel-Oulad Ogbane, Morocco (El Hamidi et al., 2021)	SEAWAT, climate/SLR to 2040	Intrusion toe ~5.2 km inland (15 - 25 g/L) under combined stress vs 3.8 km baseline (+36%)
Benin coastal aquifers (Agossou et al., 2022)	3-D SEAWAT, 2015-2020 baseline	1.65 m head decline; 1.92 km^2 intrusion-area increase over 5 yrs; recharge offsets moderate SLR

4.6. Model Reliability, Uncertainty and Appropriate Use

The calibration statistics indicate that the model reproduces the dominant head and chloride gradients, and the independent checks are broadly consistent in direction and order of magnitude with the observed head decline and coastal chloride increase reported between 2015 and 2025. Because each scenario, including the reference, is run as an independent steady-state simulation rather than a transient 2015-2025 run, this consistency check should be read as supporting plausibility, not as formal temporal validation. The unchanged ranking of scenarios by direction of response under ±20% hydraulic-conductivity and dispersivity perturbations further supports comparative use. Nevertheless, the model remains a two-dimensional representation of a heterogeneous aquifer. Fractures, dissolution features, clay lenses, pumping geometry and three-dimensional flow paths can create local behaviour that is not captured by a single section (Meyer et al., 2019).

For this reason, the most defensible interpretation is comparative rather than predictive: pumping reduction and recharge move the system in a freshwater-preserving direction, whereas higher coastal head and combined stress move it toward greater intrusion. Exact chloride values and front positions should be updated as additional lithological, pumping, monitoring-head and salinity data become available. A future three-dimensional model should reserve an independent monitoring period for out-of-sample validation.

4.7. Management Implications for the Tudor Aquifer

The modelling results support an adaptive management framework built around measurable hydraulic and water-quality indicators (**Table 6**). Groundwater licensing should be linked to cumulative abstraction rather than individual permits alone; monitoring should combine groundwater head, chloride or electrical conductivity and local coastal-water level; and managed recharge should be tested as a complementary intervention rather than a substitute for pumping control. Model updates should be scheduled when new monitoring data materially change the inferred hydraulic or salinity gradients.

Table 6. Translation of model evidence into management actions.

Model evidence	Hydrogeological interpretation	Management implication
Pumping control (−30%, to 8050 m^3/day): freshwater-preserving direction (directional response; raw Δ not reported)	Reduced withdrawal preserves inland head and seaward discharge	Meter cumulative abstraction; stage reductions where head/chloride triggers are exceeded
Managed recharge (650 mm/yr): coastal chloride reduced from 12,847 to ≈7837 mg/L (−39%); largest simulated improvement	Additional freshwater head resists saline migration	Pilot recharge inland with water-quality, clogging and mounding safeguards
Higher coastal head (+0.50 m): intrusion-worsening direction (directional response; raw Δ not reported)	Saline-side pressure reduces freshwater-to-coastal contrast	Maintain datum-consistent tide-gauge and groundwater-head monitoring
Combined stress (pumping 14,000 m^3/day; recharge −20%; coastal head +0.73 m): 5000 mg/L front 2.50 → ≈4.54 km inland (+2.04 km)	Pumping and saline boundary pressure amplify each other	Use joint pumping-recharge-coastal-head scenarios in licensing and planning

4.8. Limitations and Future Research Directions

This study has several limitations that bound the appropriate use of its results. The model is a two-dimensional representation of a single inland-to-coast transect, calibrated to a single 2025 hydrochemical campaign and eight head observations; it is therefore suited to comparative scenario testing rather than parcel-scale or fully three-dimensional prediction. The represented pumping total (11,500 m^3/day) necessarily excludes licensed abstraction outside the represented section, and the positive chloride calibration bias (+176 mg/L) indicates a modest tendency toward overprediction of salinity that should be considered when reference chloride-front positions are used for planning. Recharge was treated throughout as a calibrated model input rather than a measured Tudor water balance, given the absence of a site-specific water-balance study. Future research should prioritize a three-dimensional representation of the aquifer informed by additional borehole lithology and pumping-test data; a monitored managed-recharge pilot with paired water-quality and groundwater-mounding observations to replace the modelled recharge scenario with field-tested performance; continuous, datum-consistent tide-gauge and groundwater-head monitoring to support progressive recalibration; and formal uncertainty quantification, for example through Monte Carlo parameter sampling, to complement the deterministic scenario comparisons reported here (Agossou et al., 2022).

5. Conclusion

A calibrated two-dimensional SEAWAT model of the Tudor coastal aquifer reproduced the principal observed hydraulic-head and chloride gradients, with hydraulic-head RMSE of 0.38 m and chloride RMSE of 892 mg/L. Under the 2025 reference condition, the 5000 mg/L and 1000 mg/L isochlors occurred approximately 2.5 km and 5.5 km inland, respectively. The scenario experiments show a consistent hydraulic pattern: measures that preserve or increase freshwater head reduce intrusion, whereas higher saline-side boundary pressure and combined stress intensify inland migration.

A 30% reduction in represented pumping moved the freshwater response in the improving direction. Managed recharge produced the strongest quantified improvement, reducing coastal chloride from 12,847 mg/L to approximately 7837 mg/L (about 39% lower). A higher coastal-head condition moved the system toward greater intrusion, while combined stress (pumping 14,000 m^3/day, recharge reduced 20% to 120 mm/year, coastal head +0.73 m) caused the largest deterioration, advancing the 5000 mg/L chloride front from 2.50 km to approximately 4.54 km inland of the coast (about 2.04 km). Parameter sensitivity changed simulated chloride magnitude but not the ranking of scenarios by direction of response. Scenario-specific raw head/chloride changes not retained in the available output summary are not estimated or reconstructed here.

For management, the strongest implication is that abstraction control and carefully monitored managed recharge should be evaluated together as head-preservation measures, rather than treating pumping, recharge and sea-level change as separate management narratives. The model is appropriate for comparative decision support at aquifer scale, not parcel-scale prediction. Continued head, salinity, abstraction and tide-gauge monitoring, improved characterization of aquifer heterogeneity, and eventual three-dimensional variable-density modelling would strengthen future forecasts and management thresholds for the Tudor aquifer.

Publication Positioning

This manuscript is intentionally distinct from the authors' 2026 hydrochemical and statistical Tudor paper. The earlier article establishes field and statistical evidence of salinization, whereas the present study contributes variable-density governing equations, model discretization, calibration diagnostics, reference-state simulation, management and stress scenarios, sensitivity analysis, and model-based management testing. Shared observations are cited to the companion paper rather than presented as a second independent dataset.

Funding

This research received no specific grant from any funding agency in the public, commercial or not-for-profit sectors.

Data and Model Availability

The manuscript reports calibrated model structure, performance statistics and scenario outputs. Administrative groundwater records and tide-gauge observations remain subject to the access conditions of the respective data custodians. Model files may be shared subject to those data-governance requirements.

Acknowledgements

The authors acknowledge Kenyatta University, the Water Resources Authority and the Kenya Ports Authority for institutional, groundwater and coastal-boundary information that supported the study. The authors also acknowledge the borehole owners and field participants who facilitated groundwater investigation and monitoring access.

Author Contributions

Conceptualization, C.N.K., M.M. and S.M.; methodology, C.N.K.; software, C.N.K.; formal analysis, C.N.K.; investigation, C.N.K.; data curation, C.N.K.; writing—original draft preparation, C.N.K.; writing—review and editing, M.M. and S.M.; supervision, M.M. and S.M. All authors have read and agreed to the published version of the manuscript.

Conflicts of Interest

The authors declare no conflicts of interest regarding the publication of this paper.

References

Abd-Elaty, I., Javadi, A. A., & Abd-Elhamid, H. (2021). Management of Saltwater Intrusion in Coastal Aquifers Using Different Wells Systems: A Case Study of the Nile Delta Aquifer in Egypt. *Hydrogeology Journal, 29,* 1767-1783. https://doi.org/10.1007/s10040-021-02344-w

Agossou, A., Yang, J. S., & Lee, J. B. (2022). Evaluation of Potential Seawater Intrusion in the Coastal Aquifers System of Benin and Effect of Countermeasures Considering Future Sea Level Rise. *Water, 14,* Article 4001. https://doi.org/10.3390/w14244001

Akhtar, J., Sana, A., Tauseef, S. M., & Tanaka, H. (2022). Numerical Modeling of Seawater Intrusion in Wadi Al-Jizi Coastal Aquifer in the Sultanate of Oman. *Hydrology, 9,* Article

211. https://doi.org/10.3390/hydrology9120211

Cao, X., Guo, Q., & Liu, W. (2024). Research on the Patterns of Seawater Intrusion in Coastal Aquifers Induced by Sea Level Rise under the Influence of Multiple Factors. *Water, 16,* Article 3457. https://doi.org/10.3390/w16233457

El Hamidi, M. J., Larabi, A., & Faouzi, M. (2021). Numerical Modeling of Saltwater Intrusion in the Rmel-Oulad Ogbane Coastal Aquifer (Larache, Morocco) in the Climate Change and Sea-Level Rise Context (2040). *Water, 13,* Article 2167. https://doi.org/10.3390/w13162167

Gopinath, S., Srinivasamoorthy, K., Saravanan, K., & Prakash, R. (2019). Discriminating Groundwater Salinization Processes in Coastal Aquifers of Southeastern India: Geophysical, Hydrogeochemical and Numerical Modeling Approach. *Environment, Development and Sustainability, 21,* 2443-2458. https://doi.org/10.1007/s10668-018-0143-x

Hingst, M. C., Housego, R. M., He, C., Minsley, B. J., Ball, L. B., & Michael, H. A. (2024). Beyond the Wedge: Impact of Tidal Streams on Salinization of Groundwater in a Coastal Aquifer Stressed by Pumping and Sea-Level Rise. *Water Resources Research, 60,* e2023WR035840. https://doi.org/10.1029/2023wr035840

Intergovernmental Panel on Climate Change (2021). *Climate Change 2021: The Physical Science Basis.* Cambridge University Press.

Kenya National Bureau of Statistics (2019). *2019 Kenya Population and Housing Census: Volume I, Population by County and Sub-County.*

Kithome, C. N., Makokha, M., & Murimi, S. (2026). Quantifying Seawater Intrusion in a Stressed Coastal Aquifer Using Hydrochemical and Statistical Analysis: Evidence from the Tudor Aquifer, Kenya. *Journal of Geoscience and Environment Protection, 14,* 49-63. https://doi.org/10.4236/gep.2026.145005

Llopis-Albert, C., & Pulido-Velázquez, D. (2014). Discussion about the Validity of Sharp-Interface Models to Deal with Seawater Intrusion in Coastal Aquifers. *Hydrological Processes, 28,* 3642-3654. https://doi.org/10.1002/hyp.9908

Makokha, M. (2019). Groundwater Quality Analyses along Kenyan Coastal Region, Case Study of Kilifi-Kenya. *International Journal of Environment and Geoinformatics, 6,* 1-14. https://doi.org/10.30897/ijegeo.466933

Mantoglou, A. (2003). Pumping Management of Coastal Aquifers Using Analytical Models of Saltwater Intrusion. *Water Resources Research, 39,* 2002WR001891. https://doi.org/10.1029/2002wr001891

Meyer, R., Engesgaard, P., & Sonnenborg, T. O. (2019). Origin and Dynamics of Saltwater Intrusion in a Regional Aquifer: Combining 3-D Saltwater Modeling with Geophysical and Geochemical Data. *Water Resources Research, 55,* 1792-1813. https://doi.org/10.1029/2018wr023624

Mtoni, Y., Mjemah, I. C., Bakundukize, C., Van Camp, M., Martens, K., & Walraevens, K. (2013). Saltwater Intrusion and Nitrate Pollution in the Coastal Aquifer of Dar es Salaam, Tanzania. *Environmental Earth Sciences, 70,* 1091-1111. https://doi.org/10.1007/s12665-012-2197-7

Narayanan, D., & Eldho, T. I. (2024). Potential Impacts of Saline Groundwater Pumping on Seawater Intrusion in a Coastal Aquifer System. *ISH Journal of Hydraulic Engineering, 30,* 511-521. https://doi.org/10.1080/09715010.2024.2366454

Oiro, S., & Comte, J. C. (2019). Drivers, Patterns and Velocity of Saltwater Intrusion in a Stressed Aquifer of the East African Coast: Joint Analysis of Groundwater and Geophysical Data in Southern Kenya. *Journal of African Earth Sciences, 149,* 334-347. https://doi.org/10.1016/j.jafrearsci.2018.08.016

Pool, M., & Carrera, J. (2011). A Correction Factor to Account for Mixing in Ghyben-Her-

zberg and Critical Pumping Rate Approximations of Seawater Intrusion in Coastal Aquifers. *Water Resources Research, 47,* 2010WR010256.
https://doi.org/10.1029/2010wr010256

Republic of Kenya (2016). *Water Act, No. 43 of 2016.* Government Printer.

Tran, D. A., Tsujimura, M., Pham, H. V., Nguyen, T. V., Ho, L. H., Le Vo, P. et al. (2022). Intensified Salinity Intrusion in Coastal Aquifers Due to Groundwater Overextraction: A Case Study in the Mekong Delta, Vietnam. *Environmental Science and Pollution Research, 29,* 8996-9010. https://doi.org/10.1007/s11356-021-16282-3

Water Resources Authority (2025). *Tudor Aquifer Borehole, Licensed-Abstraction, Groundwater-Level and Chloride Records, 2015-2025* [Administrative Dataset].

Werner, A. D., Bakker, M., Post, V. E. A., Vandenbohede, A., Lu, C., Ataie-Ashtiani, B. et al. (2013). Seawater Intrusion Processes, Investigation and Management: Recent Advances and Future Challenges. *Advances in Water Resources, 51,* 3-26.
https://doi.org/10.1016/j.advwatres.2012.03.004